ELSEVIER

Journal of Molecular Catalysis A: Chemical 163 (2000) 129–145

JOURNAL OF MOLECULAR CATALYSIS A: CHEMICAL

www.elsevier.com/locate/molcata

# Oxametallacycle formation via ring-opening of 1-epoxy-3-butene on Ag(1 1 0): a combined experimental/theoretical approach

J. Will Medlin [a], Mark A. Barteau [a,*], John M. Vohs [b]

[a] *Center for Catalytic Science and Technology, Department of Chemical Engineering, University of Delaware, Newark, DE 19716, USA*
[b] *Department of Chemical Engineering, University of Pennsylvania, Philadelphia, PA 19104, USA*

Received 2 February 2000; accepted 1 April 2000

**Abstract**

Temperature-programmed desorption (TPD), high resolution electron energy loss spectroscopy (HREELS), and density functional theory (DFT) calculations were used to study the interaction of 1-epoxy-3-butene (EpB) with the Ag(1 1 0) surface. The goal of this study was to better understand the nature of the strongly adsorbed EpB species reported for the silver-catalyzed butadiene epoxidation process. EpB dosed on the Ag(1 1 0) surface at 300 K ring-opens to form a stable surface oxametallacycle intermediate. DFT geometry optimizations were utilized to calculate the structure of the oxametallacycle; subsequent frequency calculations were used to predict the vibrational spectrum of this intermediate. Comparison of the predicted vibrational spectrum with the experimental HREEL spectrum of this intermediate conclusively identifies the oxametallacycle. This oxametallacycle undergoes 1,2- and 1,4-ring-closure reactions during TPD to form EpB and 2,5-dihydrofuran (2,5-DHF), respectively. This reaction represents the first demonstration of a surface oxametallacycle ring-closure to form an epoxide, and thus we suggest that the strongly adsorbed surface intermediate in the butadiene epoxidation process is a surface oxametallacycle. Furthermore, in light of the similarity between butadiene epoxidation and other epoxidation processes, surface oxametallacycles may be of general importance in silver-catalyzed olefin epoxidation. 

*Keywords:* TPD; 1-Epoxy-3-butene (EpB); Density functional theory; HREELS; Oxametallacycle

## 1. Introduction

Silver-catalyzed olefin epoxidation continues to be an important industrial process. Ethylene oxide (EO) generated by ethylene epoxidation has long been among the largest volume chemicals produced by the chemical industry [1]. Recently, the commercialization of a butadiene epoxidation process for production of 1-epoxy-3-butene (EpB) has focused increased attention on olefin epoxidation reactions [2]. Ethylene and butadiene epoxidation processes both employ silver catalysts supported on $\alpha$-$Al_2O_3$ and promoted by alkalis and halides.

Considerable work has been devoted to understanding the mechanism of silver-catalyzed epoxidation reactions, especially for ethylene epoxidation [3,4]. It is now generally accepted that *atomic* (rather than molecular) adsorbed oxygen adds to ethylene in the rate determining step to form ethylene oxide [5]. Studies on model silver surfaces have shown that styrene [6], norbornene [7], and 3,3-dimethylbutene [8] are also epoxidized by atomic oxygen; again, addition of atomic oxygen to the olefin function is rate-limiting. Because subsequent steps are rapid, little has been

* Corresponding author. Tel.: +1-302-831-8905; fax: +1-302-831-8201.
*E-mail address:* barteau@che.udel.edu (M.A. Barteau).

1381-1169/00/$ – see front matter 
PII: S1381-1169(00)00406-4

learned of the nature of the organic intermediate(s) formed during olefin epoxidation. Studying the mechanism of ethylene epoxidation, in particular, is difficult using ultrahigh vacuum (UHV) surface science techniques. The interaction of ethylene with silver surfaces under UHV conditions is too weak to allow direct study of the mechanism of ethylene epoxidation; furthermore, ethylene oxide desorbs without reacting during temperature programmed desorption on silver surfaces, making study of the reverse reaction similarly problematic [9]. Studies of organic intermediates important in ethylene epoxidation have largely relied on using indirect methods, e.g. synthesis of likely surface intermediates from halohydrins [10].

Butadiene epoxidation is a unique candidate for study using surface science techniques. In contrast to ethylene epoxidation, it has been proposed that the rate of butadiene epoxidation may be limited by desorption of the product EpB [11]. This scenario would suggest that a strongly bound intermediate is present on the catalyst surface; due to its strongly bound nature, it should be possible to study this intermediate using surface science techniques to probe its structure and reactivity. Because of the similarities between epoxidation processes, understanding the mechanism of EpB formation may provide insights into the mechanisms and intermediates of importance in other olefin epoxidation reactions, including ethylene epoxidation.

One species proposed as a possible intermediate for olefin epoxidation is the surface oxametallacycle. This species, which contains the –O–C–C– linkage tethered at both ends to surface metal atoms, has been proposed as an intermediate in reactions of various oxygenates on transition metal surfaces, including reactions involving epoxides [12–17]. Total energy calculations using density functional theory (DFT) have demonstrated that oxametallacycles on silver are modestly stable with respect to elimination of gas phase epoxides, indicating that oxametallacycles are energetically feasible structures along the reaction coordinate of olefin epoxidation [18,19]. It has proven difficult, however, to isolate and study oxametallacycle intermediates experimentally. The first isolation and spectroscopic identification of a stable oxametallacycle was recently reported [10] for the reaction of 2-iodoethanol on Ag(1 1 0). During TPD experiments, this oxametallacycle reacted to form γ-butyrolactone (GBL) and acetaldehyde as major products. DFT frequency calculations used to identify the oxametallacycle predicted a vibrational mode at 717 $cm^{-1}$ which appeared to represent the reaction coordinate for ring closure to form ethylene oxide. However, no direct experimental link between the oxametallacycle intermediate and ethylene oxide formation was found. Thus, the question remains: can oxametallacycles react via ring closure to form epoxides? Or, stated another way, are these species intermediates in the synthesis of epoxides from olefins, or in the degradation of epoxides to other, often less desirable, products?

As part of a continuing effort to understand the mechanism of olefin epoxidation, we have recently focused on exploring intermediates of potential importance in the butadiene epoxidation process. Previous surface science studies by Roberts et al. [20] examined the reaction of butadiene with atomic oxygen on the Ag(1 1 0) surface. They found that EpB is not produced from butadiene oxidation under UHV conditions, in contrast to the commercially practiced reaction on silver catalysts [11]. Instead, oxygen reacts by 1,4-addition to butadiene to form 2,5-dihydrofuran and furan as the major products in UHV. Epoxidation of butadiene was not observed under the experimental conditions of that study, and there has been no previous surface science study of the interaction of the epoxidation product, EpB, with silver. In particular, the nature of the strongly bound adsorbed EpB state reported for the industrial supported catalyst is not well understood. In the present study, we have used temperature-programmed desorption (TPD) and high resolution electron energy loss spectroscopy (HREELS), along with DFT-based ab initio calculations, to study the interaction of EpB with the Ag(1 1 0) surface.

We report here the isolation and spectroscopic identification of a stable oxametallacycle intermediate during the reaction of EpB on Ag(1 1 0). We believe this represents the first conclusive link between a stable oxametallacycle intermediate and a gas-phase epoxide. This oxametallacycle is a strongly bound species, but reacts at high temperature to produce EpB and 2,5-DHF. The experimental and theoretical results described below suggest that the strongly bound surface intermediate reported for the butadiene epoxidation process may be an oxametallacycle, and imply that oxametallacycles are potentially important intermediates in olefin epoxidation processes, in gen-

eral. Also presented below are the experimental and theoretical vibrational spectra used in identifying the oxametallacycle intermediate, as well as energetics for this first example of oxametallacycle ring closure to form a free epoxide, in this case EpB.

## 2. Experimental

All experiments were performed in one of two ultrahigh vacuum (UHV) chambers. TPD experiments were performed in a chamber which has been described previously [21]. The system was evacuated to a base pressure of $1 \times 10^{-10}$ Torr by a combination of diffusion and ion pumps. The chamber was equipped with a sputter ion gun for sample cleaning, four-grid optics for LEED and AES experiments, and a UTI 100C quadrupole mass spectrometer for TPD experiments. Products desorbed during TPD experiments were identified by deconvolution of the contributions of mass fragments for each product. Product mass fragmentation patterns were determined experimentally, by backfilling the system with the pure component.

High resolution electron energy loss (HREELS) experiments were carried out in a second UHV chamber which has been described previously [22]. The system was evacuated to a base pressure of $1 \times 10^{-10}$ Torr using a combination of ion and turbomolecular pumps. The chamber was equipped with an LK Technologies ELS 3000 spectrometer for HREELS experiments. All HREEL spectra were collected in the specular direction with the electron beam incident 60° from the surface normal. All spectra were obtained using a full width at half-maximum (FWHM) resolution of 3–3.5 meV for the elastically scattered beam at an electron beam energy of 3 eV. The system was also equipped with LEED and AES capabilities.

The silver single crystal was aligned to the (1 1 0) orientation using the Laue method and polished using standard metallographic techniques. The (1 1 0) surface orientation was verified using LEED. In both systems, the Ag(1 1 0) sample was mounted on a tantalum foil backing plate which was spot welded to two tantalum wires. Resistive sample heating was accomplished by passing current through the tantalum wires. Impurities were removed from the fresh crystal surface by successive cycles of argon-ion bombardment followed by annealing at 1000 K. Surface cleanliness was verified using oxygen TPD or HREELS. Epoxybutene (Eastman Chemical, 99%) was purified by repeated freeze-pump-thaw cycles and stored in glass dosing tubes.

Absolute product yields from TPD experiments were determined using the method described by Ko et al. [23] for correction of peak areas using mass spectrometer sensitivity factors. A p(3×1) oxygen-covered surface was used to provide a standard 0.33 monolayer (ML) reference using previously described methods [24].

## 3. Computational details

The Amsterdam density functional (ADF) program [25–27] was used as described previously [18] to determine the fully optimized geometry of EpB oxametallacycles adsorbed onto Ag clusters. ADF was also used to calculate the infrared vibrational spectra of optimized oxametallacycle structures. ADF represents molecular orbitals as linear combinations of atomic Slater-type orbitals, and solves Kohn–Sham one-electron equations using the Vosko–Wilk–Nusair (VWN) functional [28]. Unless noted otherwise, all calculations were spin-unrestricted and employed the Becke [29] and Perdew [30] gradient approximations for the exchange and correlation energy terms, respectively. Double-zeta basis sets were utilized for all computations, except where noted otherwise. To obtain estimates for vibrational spectra, two-point frequency calculations using an integration accuracy of $10^{-6}$ were performed on optimized EpB oxametallacycles. The resulting frequencies were then scaled by a factor $x$, where $0.96 \leq x \leq 1.03$, to improve alignment with experimental data. Energies (or stability values) were calculated for oxametallacycle formation from EpB plus the bare metal center according to

$$\Delta H_{\mathrm{rxn}} \approx \Delta E_{\mathrm{rxn}} = E(\text{oxametallacycle}) - \{E(\mathrm{EpB}) + E(\mathrm{M}_n)\} \quad (1)$$

where $E$(EpB) and $E(\mathrm{M}_n)$ are the respective total energies of the free epoxide and the bare metal cluster consisting of $n$ atoms of metal M.

## 4. Results

### 4.1. Temperature-programmed desorption

Epoxybutene adsorbed onto the clean Ag(1 1 0) surface at 120 K desorbs in two peaks at 165 and 215 K. Fig. 1(a) shows the $m/e = 70$ spectrum used to track EpB desorption for a representative TPD experiment.

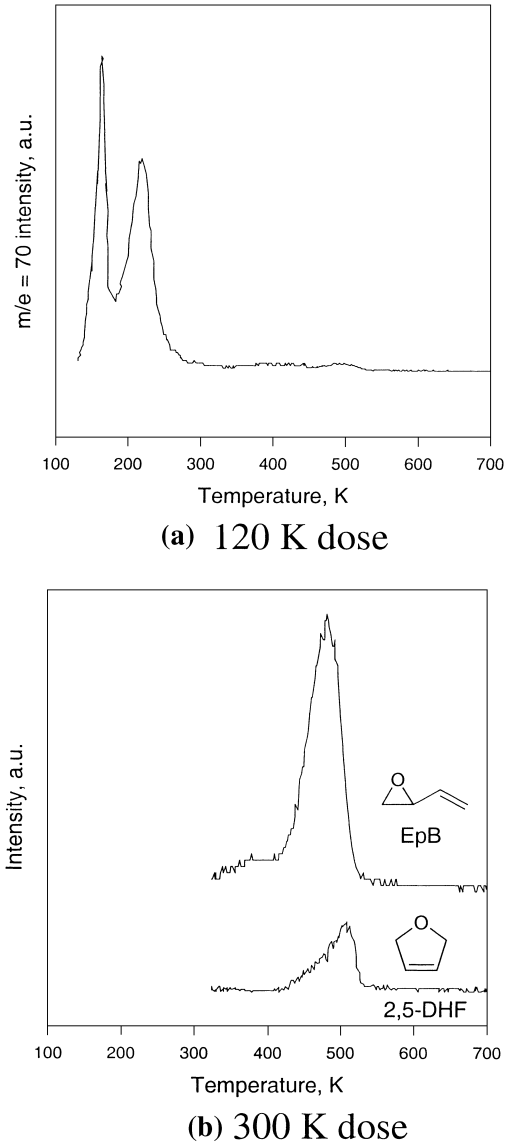


Fig. 1. TPD spectra after EpB dose to Ag(1 1 0): (a) $m/e = 70$ spectrum (used to track EpB desorption) after 120 K dose; (b) corrected product desorption spectra after 300 K dose.

Variation of the EpB exposure prior to TPD reveals that the 165 K peak does not saturate for larger doses; this peak is, therefore, attributed to the desorption of EpB multilayers. The 215 K peak becomes saturated at ca. 0.5 ML for high EpB exposures, and is attributed to desorption of surface-bound EpB. This saturation coverage is in agreement with that observed for ethylene oxide and propylene oxide on Ag(1 1 0) [31]. There is also a very small feature in the TPD spectrum at 490 K. For these TPD experiments, however, the intensity of the 490 K peak is too low to permit the identification of any desorbed products.

TPD experiments were also performed after EpB was dosed to the Ag(1 1 0) surface at 300 K. These higher temperature exposures result in a much larger EpB desorption peak at 490 K. A small amount of 2,5-dihydrofuran (2,5-DHF) also desorbs in a peak centered at 510 K. Fig. 1(b) shows a representative TPD spectrum following a 70% saturation EpB dose. EpB and 2,5-DHF were identified as products by comparing their pure component mass fragmentation patterns to the mass spectra observed in the TPD experiments; in general, 25 representative masses were monitored during each TPD run. Crotonaldehyde, 2,3-DHF, furan, and other compounds with similar fragmentation patterns were also considered, but were ruled out as products based on key differences between their relative mass fragment intensities and those of the desorbed products. The root mean square (rms) error associated with product assignment was determined by calculating the percent error between the experimental TPD peak areas and those predicted based on the fragmentation patterns of both products for all 25 representative masses. The rms error associated with assigning the observed mass spectra to the products EpB and 2,5-DHF was found to be approximately 2%.

Increasing the EpB exposure prior to TPD results in an increase in the amount of EpB and 2,5-DHF desorbed at high temperature, until the desorption peaks become saturated at a coverage corresponding to 0.47 monolayers. As the EpB exposure prior to TPD is increased, the selectivity to EpB also increases, to a value of 82% at saturation coverage. Fig. 2 shows the relationship between coverage and selectivity to EpB. The high temperature at which these two products desorb indicates that a strongly bound intermediate is formed by EpB adsorption on Ag(1 1 0) at 300 K. When adsorbed at low temperature

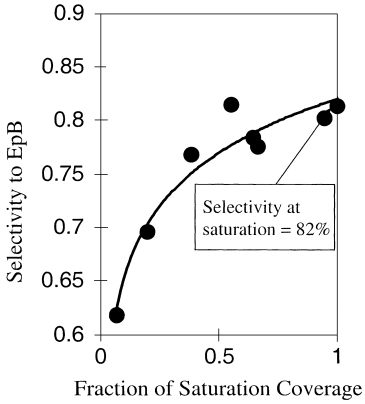


Fig. 2. Selectivity to EpB during TPD as a function of coverage of strongly bound intermediate, after 300 K dose. Here, a fractional coverage of 1 corresponds to the saturation coverage, 0.47 ML.

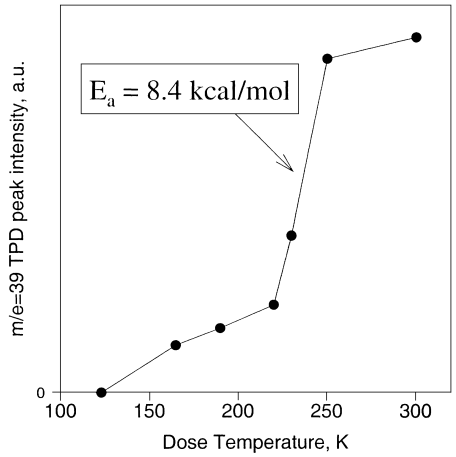


Fig. 3. Integrated TPD peak intensity for $m/e = 39$ (representative of EpB and 2,5-DHF) as a function of prior EpB dose temperature.

(<200 K), molecular EpB desorbs at 215 K; 2,5-DHF adsorbed on Ag(1 1 0) desorbs at 250 K [20]. Moreover, it is unlikely that any intact adsorbed molecule would be stable at temperatures above 400 K. This suggests that some other strongly bound intermediate is responsible for formation of the high temperature EpB and 2,5-DHF products. As evidenced by the extremely low 490 K peak intensity in Fig. 1(a), the strongly bound EpB intermediate is not formed in appreciable amounts when EpB is adsorbed at 120 K, indicating that there is a significant activation energy for its formation. This activation energy requirement implies that some bond within the original molecule must be broken and other bonds formed to the surface to create this intermediate.

In order to evaluate the activation energy for formation of the strongly adsorbed EpB intermediate, a series of experiments was performed in which equal exposures of EpB to the Ag(1 1 0) surface were made over a range of temperatures from 120–300 K. Subsequent to each exposure, a TPD experiment was carried out to determine the amount of EpB and 2,5-DHF products which desorbed at high temperature from reaction of the strongly bound intermediate. Fig. 3 shows a plot of the integrated high temperature peak intensity versus the temperature of EpB adsorption. The data collected at exposure temperatures $\geq$220 K were fit to a kinetic model for formation of the intermediate. On the basis of the assumption that there are no competing reaction channels for EpB above 215 K, the following model expression was used to describe the reaction kinetics:

$$\frac{\mathrm{d}\theta}{\mathrm{d}t} = kP_{\mathrm{EpB}}(1-\theta) \tag{2}$$

where $\theta$ is the fractional coverage of the strongly bound EpB intermediate, and where $P_{\mathrm{EpB}}$, the partial pressure of EpB, was assumed to be constant during the dose. This model assumes a first order dependence in both EpB partial pressure and vacant surface sites. By integrating (2), and assuming an Arrhenius expression for the rate constant $k$, one can develop the following equation

$$\ln\left(\ln\left[\frac{1}{1-\theta}\right]\right) = \ln(AP_{\mathrm{EpB}}\Delta t) - \frac{E_{\mathrm{A}}}{RT} \tag{3}$$

where $A$ is the pre-exponential factor for the activated adsorption process, $\Delta t$ the exposure time, and $E_{\mathrm{A}}$ the activation energy. Thus, a plot of the left hand side of Eq. (3) versus $1/T$, where $T$ is the exposure temperature, should produce a straight line with slope $= -E_{\mathrm{A}}/R$. Performing this analysis of the data in Fig. 3 yields an apparent activation energy of $8.4 \pm 0.5$ kcal/mol.

As mentioned above, this activation energy requirement is consistent with the hypothesis that at least one bond in EpB must be broken for the strongly bound intermediate to be formed. Cleavage of one of the C–C bonds of EpB would likely lead to the production of lower molecular weight products, which is inconsistent with the observation that EpB and

2,5-DHF are the only major reaction products. Similarly, cleavage of one or more C–H bonds would likely result in the formation of dehydrogenated products, e.g. furan. Another possibility is that a C–O bond on one side of the epoxide ring is broken. Cleavage of a single C–O bond would result in the formation of a surface oxametallacycle; this intermediate could subsequently react to form products that maintain the molecular weight of EpB. To determine the nature of the strongly bound EpB intermediate, however, surface spectroscopic techniques are necessary.

### *4.2. High resolution electron energy loss spectroscopy*

In order to determine the identity of the intermediates involved in the interaction of EpB with Ag(1 1 0), a series of HREELS experiments was performed on this system. First, EpB was adsorbed on the Ag(1 1 0) surface at 140 K, then maintained below 130 K for HREELS analysis. The resulting spectrum is shown as Fig. 4(a). Based on a comparison with the IR vibrational spectrum of liquid-phase EpB collected by this laboratory, the species present at 140 K can clearly be identified as molecular EpB multilayers, as indicated by the TPD results described above. The assignments of observed vibrational modes are listed in Table 1. Descriptions of the vibrational modes were obtained by viewing animations of normal modes predicted by DFT-based frequency calculations of the fully optimized geometry of the EpB molecule. The DFT results and mode assignments are discussed in a subsequent section.

In a separate experiment, EpB was adsorbed on the Ag(1 1 0) surface at 190 K, then maintained below 170 K for HREELS investigation. The resulting spectrum is shown as Fig. 4(b). In this spectrum, most of the major energy loss peaks from the 140 K dose are still readily discernible, including the major features at 806, 917, and 996 $cm^{-1}$. However, several new features have also appeared, most notably peaks at 400, 720, and 849 $cm^{-1}$. The appearances of these new peaks in the HREEL spectrum indicate that some new intermediate has been formed during the 190 K adsorption of EpB. Moreover, the persistence of spectral features associated with molecular EpB suggests that EpB is coadsorbed with this new intermediate for the 190 K EpB dose.

In order to isolate and study the new intermediate, EpB was dosed to the Ag(1 1 0) crystal at 300 K. For this experiment, the crystal was maintained at room temperature for HREELS analysis. The resulting spectrum is shown as Fig. 4(c). In this spectrum, the energy loss peaks from the EpB multilayer spectrum of Fig. 4(a) have disappeared entirely. Only peaks which correspond to the new intermediate remain, indicating that this new intermediate has been isolated at 300 K. This result is in agreement with our TPD results, which showed that intact adsorbed EpB desorbs from Ag(1 1 0) by 215 K. Thus the spectrum shown in Fig. 4(c) corresponds to the strongly adsorbed EpB intermediate responsible for the 490 K products in TPD. HREELS analysis confirms that the strongly bound intermediate is not merely adsorbed intact EpB. The spectra obtained after adsorption at 140 and 300 K are measurably different, indicating substantial differences in the structure of the species isolated at these temperatures. Comparison of the spectrum for the strongly bound EpB intermediate with a DFT-calculated vibrational spectrum for an oxametallacycle intermediate conclusively identifies the species isolated at 300 K as a surface oxametallacycle. The DFT-based frequency calculation results used to identify the strongly bound EpB intermediate as an oxametallacycle are discussed in the following section.

### *4.3. Density functional theory calculations*

DFT-based geometry optimization and frequency calculation techniques were utilized to study the structures of possible oxametallacycle intermediates in the reaction of EpB on Ag(1 1 0). Although oxametallacycles have been proposed as intermediates for numerous reactions [12–15,17,32–36], the only previous spectroscopic identification of a stable surface oxametallacycle intermediate was for the reaction of 2-iodoethanol on Ag(1 1 0) [10]. The oxametallacycle characterized in that study was shown to have the structure:

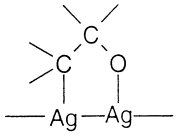


This structure, which incorporates two metal atoms to form a 5-membered oxametallacycle ring, is referred

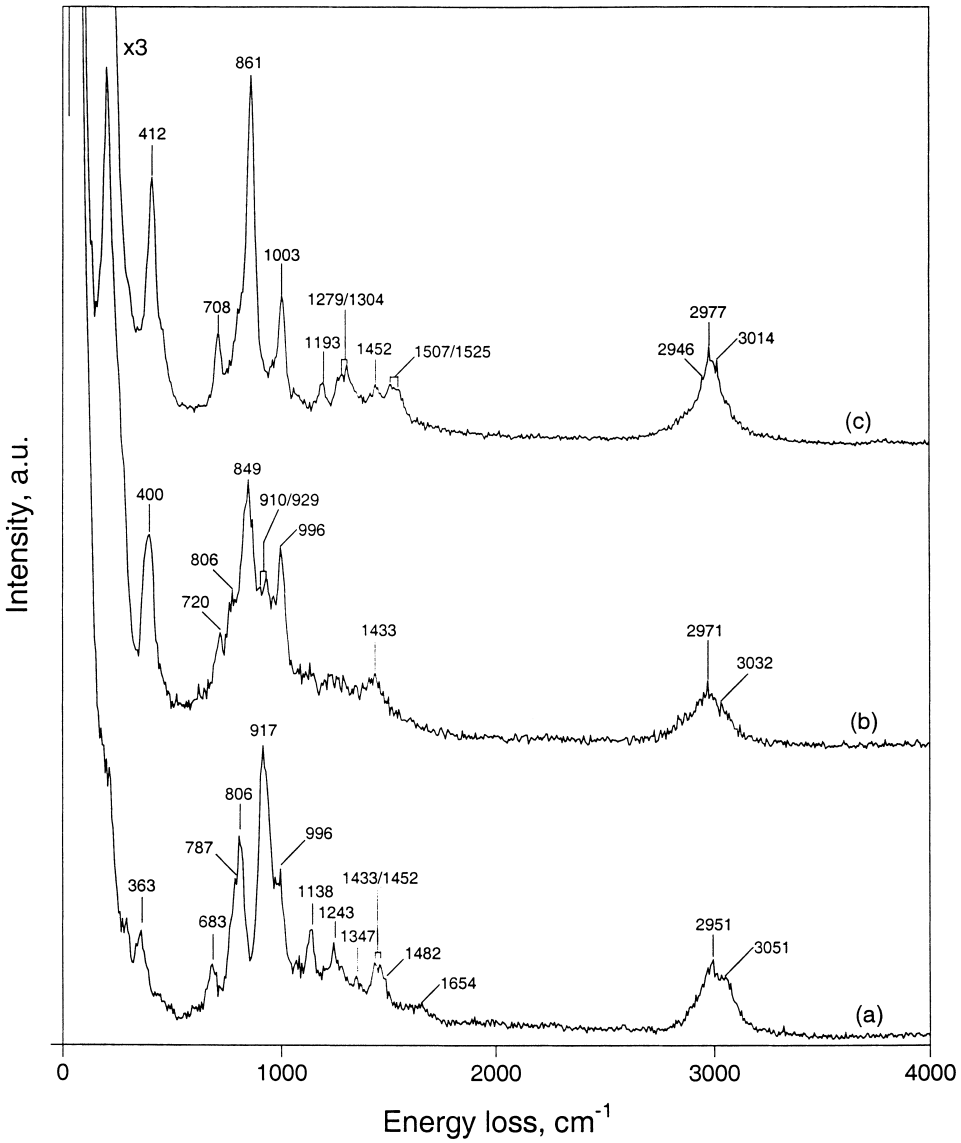


Fig. 4. HREEL spectra collected after exposing EpB to Ag(1 1 0) at varying dose temperatures: (a) 140 K; (b) 190 K; (c) 300 K.

to as the OMME structure. In the present study, oxametallacycles incorporating a single metal atom in a 4-membered ring, i.e.

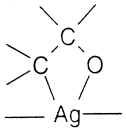


are also considered. This structure is referred to as the OME structure. Previous investigations [18,19] have shown OMMEs and OMEs to be energetically similar. Surface spectroscopic methods are therefore necessary to determine which type of oxametallacycle intermediate, if any, is formed from different reagents.

EpB oxametallacycles are formed hypothetically by insertion of a metal (in this case, silver) atom or cluster into a C–O bond of the EpB molecule. For initial calculations we performed geometry optimizations and

Table 1
Vibrational mode assignments and frequency table for molecular EpB[a]

| Mode | Liquid EpB | EpB on Ag(1 1 0) | DFT predicted |
|---|---|---|---|
| $\tau(C^2–C^3)$ | | 363 | 330 |
| $t\omega(C^4H_2)$ | 676 | 683 | 665 |
| $\delta_a(O–C^1–C^2)$ | 787 | 787 | 775 |
| $\delta_S(O–C^1–C^2)$ | 815 | 806 | 799 |
| $t\omega(C^1H_2)$ | 915 | 917 | 910 |
| $\rho(C^4H_2)$ | 915 | 917 | 918 |
| $b(C^3H)$ | 988 | 996 | 980 |
| $\rho(C^1H_2)$ | 1131 | 1138 | 1118 |
| $\nu(C^1–C^2)$ | 1243 | 1243 | 1232 |
| $\chi(C^4H_2)$ | 1343 | 1347 | 1338 |
| $\chi(C^4H_2)$ | 1440 | 1433/1452 | 1432 |
| $\chi(C^1H_2)$ | 1475 | 1482 | 1473 |
| $\nu(C^3–C^4)$ | 1644 | 1654 | 1647 |
| $\nu_S(C^1–H)/\nu_a(C^1–H)$ | 2918 | 2951 | 3020/3116 |
| $\nu_S(C^4–H)/\nu_a(C^4–H)$ | 2918 | 2951 | 3055/3179 |
| $\nu(C^2–H)/\nu(C^3–H)$ | 2995 | 3051 | 3082/3091 |

[a] $\tau$: torsion; $t\omega$: twist; $\delta_a$: asymmetric deformation; $\delta_S$: symmetric deformation; $\rho$: rock; $b$: bend; $\nu$: stretch; $\chi$: scissors; $\omega$: wag.

frequency calculations for oxametallacycles adsorbed to metal dimers and single metal atoms; previous studies have shown small cluster calculations for oxametallacycles to be in good agreement with computations involving relatively large clusters [10,18]. Selected calculations involving larger metal clusters have also been performed, and are described below. Insertion of the silver cluster into the two different ends of the epoxide ring results in the formation of two different isomers, referred to here as isomers 1 and 2. Isomer 1 is formed by insertion of a metal cluster into the vinyl-substituted end of the epoxide ring to form a linear oxametallacycle structure, shown schematically in Fig. 5(a) and (c).

Isomer 2 is produced by insertion of a metal cluster into the unsubstituted end of the epoxide ring to form a branched oxametallacycle configuration, shown as Fig. 5(b) and (d). Both types of isomers are considered as potential EpB oxametallacycle intermediates here. As a further complication, multiple energy minima have been found for each oxametallacycle structure; the results presented here correspond to the most stable geometry found for each of the isomers.

Fig. 5 also summarizes calculated stability values for EpB-derived OMMEs and OMEs, where M = Ag. Consistent with previous results for oxametallacycles, stability differences between OMMEs and OMEs are small. Isomer 1, however, is clearly the more stable isomer for both OMMEs and OMEs. In the absence of kinetic limitations, isomer 1 structures are therefore expected to be preferentially formed in reactions involving EpB oxametallacycles. We have proposed that the energetic preference for isomer 1 is due to a higher degree of conjugation of the C–C double bond [19]. The EpB OME isomer 1 configuration has been found to be the most energetically favorable structure, but all of the structures depicted in Fig. 5 are energetically feasible.

To obtain a first approximation of the vibrational spectra of EpB oxametallacycles, frequency calculations were performed for all oxametallacycles in Fig. 5. The calculated IR spectra for all 4 configurations are shown as Fig. 6. There are clearly distinguishable differences between the predicted vibrational spectra of the different oxametallacycle structures. By comparing these theoretical spectra to experimental HREEL spectra, it should be possible to distinguish which oxametallacycle geometry best corresponds to the structure of the intermediate synthesized on the surface. Thus, the computed oxametallacycle spectra of Fig. 6 were compared to the HREEL spectrum obtained after dosing EpB to Ag(1 1 0) at 300 K; as discussed above, this HREEL spectrum corresponds to the "strongly bound" EpB intermediate. This comparison clearly indicates that OME isomer 1 is the preferred oxametallacycle structure; this result is consistent with this structure having the lowest energy. Fig. 7 shows the comparison between the DFT-predicted vibrational spectrum for the EpB OME isomer 1 structure and the experimentally measured spectrum of the strongly adsorbed intermediate. In general, there is very good agreement between the two spectra. Theory accurately predicts the most intense vibrational mode at ca. 861 $cm^{-1}$, as well as the shoulder at 818 $cm^{-1}$ and the feature at 1003 $cm^{-1}$. Other modes, including those at 1200–1500 $cm^{-1}$, are represented reasonably well. The calculated C–H stretches centered near 3000 $cm^{-1}$ are slightly too low in frequency, but agreement with experiment is reasonable. The noticeable discrepancy between the experimental and theoretical spectra is in the intense feature observed experimentally at 412 $cm^{-1}$, but calculated theoretically to be 539 $cm^{-1}$. Nevertheless, agreement between the experimental and theoretical vibrational spectra is quite

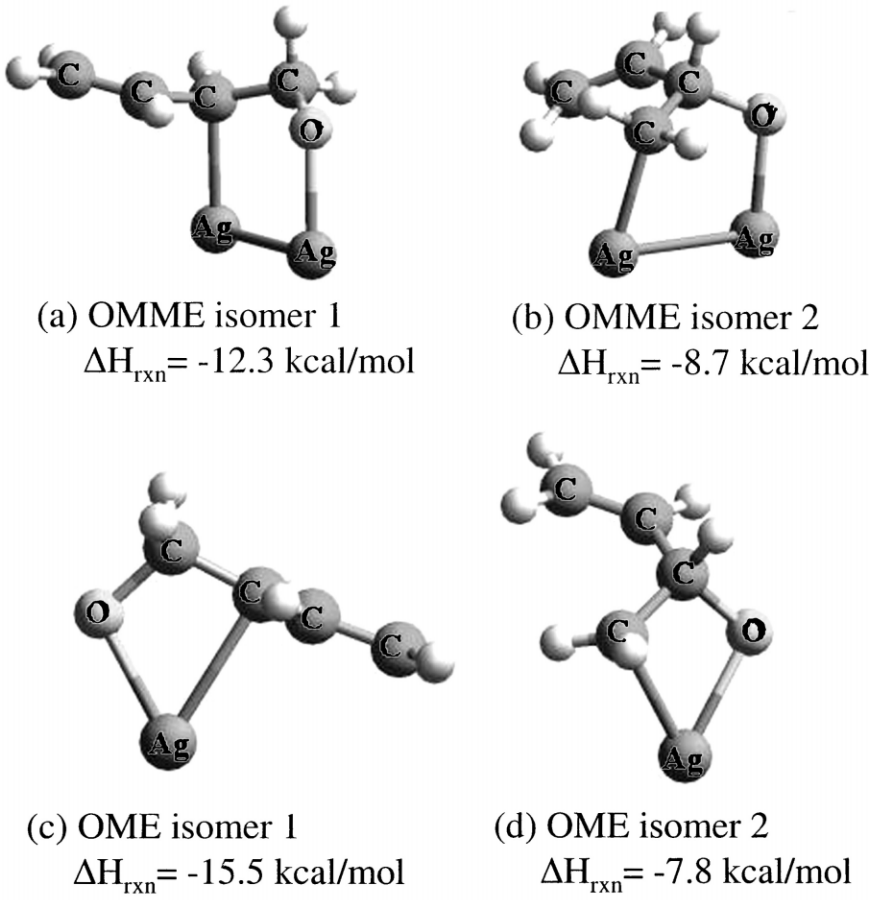


Fig. 5. Optimized structures of EpB oxametallacycles: (a) OMME isomer 1; (b) OMME isomer 2; (c) OME isomer 1; (d) OME isomer 2.

good overall, especially considering that only a single silver atom is used in the calculations to approximate an extended metal surface. In particular, the use of a single silver atom cannot be expected to capture interactions between the vinyl group and the surface.

In order to better understand possible interactions of the vinyl group with the silver surface, and in an attempt to improve agreement between theoretical and experimental vibrational spectra, DFT-based calculations were extended to oxametallacycles adsorbed on larger metal clusters. Fig. 8 shows the fully optimized structure and stability value of an EpB oxametallacycle on a 7-atom truncation of the Ag(1 1 0) surface. Increasing the silver cluster size to 7 atoms significantly stabilizes the oxametallacycle with respect to the EpB OME, to a stability value of −28.5 kcal/mol. Larger cluster calculations have also been performed on 12-atom truncations of the Ag(1 1 0) surface. The stability of the EpB OME on the 12-atom cluster has been found to be −27.3 kcal/mol, in good agreement with the 7-atom cluster result. These high stability values indicate that the EpB oxametallacycle is a *strongly bound* intermediate, in agreement with our experimental observations. These larger cluster calculations also give a clearer view of the structure of the EpB oxametallacycle on a Ag(1 1 0) surface. The details of this structure, and how they may affect oxametallacycle stability and chemistry, are considered in a subsequent section.

DFT frequency calculations were also performed for the optimized oxametallacycle structure of Fig. 8. Two sets of these calculations were performed: in

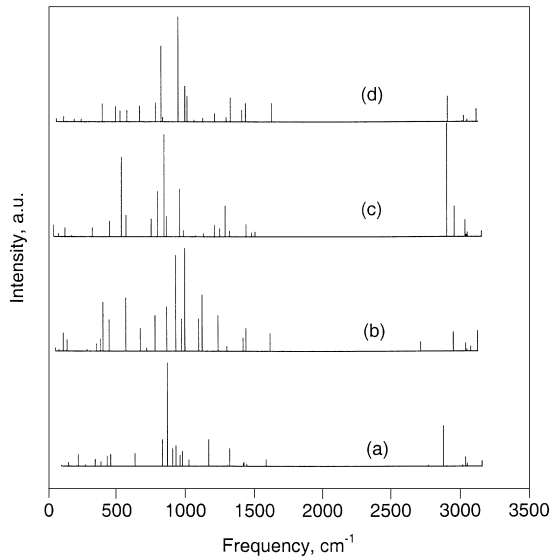


Fig. 6. Calculated IR vibrational spectra of oxametallacycles in Fig. 5: (a) OMME isomer 1; (b) OMME isomer 2; (c) OME isomer 1; (d) OME isomer 2.

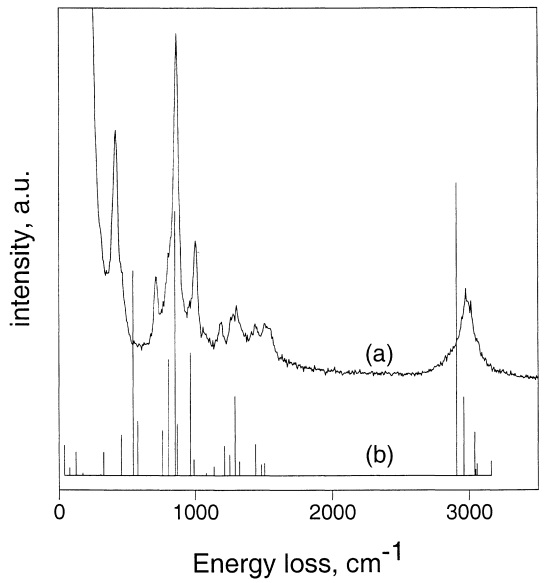


Fig. 7. Comparison between (a) HREEL spectrum collected after EpB exposure to Ag(1 1 0) at 300 K; and (b) IR spectrum calculated for the EpB OME isomer 1 structure.

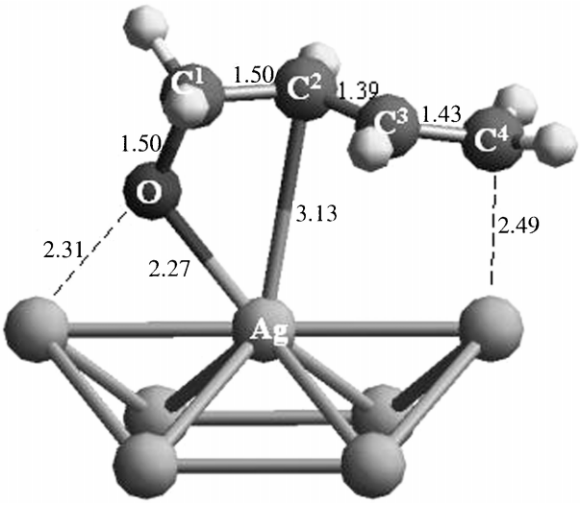


Fig. 8. Structure of optimized EpB oxametallacycle on 7-atom truncation of the Ag(1 1 0) surface. Bond distances are indicated in Angstroms.

the first, the positions of the silver atoms were held fixed; in the other, the silver atoms were allowed to vibrate. Fig. 9 shows a comparison between the DFT-predicted IR spectrum for the fixed cluster calculation and the experimental HREEL spectrum observed for the highly stable EpB intermediate isolated at 300 K. The agreement between the theoretical and experimental spectra is quite good, and clearly identifies the strongly bound epoxybutene intermediate as a surface oxametallacycle. The most intense energy losses observed experimentally, at 412, 861, 1003, and 2977 $cm^{-1}$, are all predicted with a remarkable degree of accuracy. Vibrational mode assignments for the EpB oxametallacycle are listed in Table 2, along with a comparison of fixed and non-fixed 7-atom cluster frequency calculations. Calculations incorporating larger silver cluster sizes would be expected to improve the optimized structure of the oxametallacycle, as well as the agreement between theoretical and experimental vibrational spectra; these calculations are not considered here due to their computational intensiveness.

## 5. Vibrational mode assignments

The vibrational mode assignments listed in Tables 1 and 2 were determined from viewing animations of the

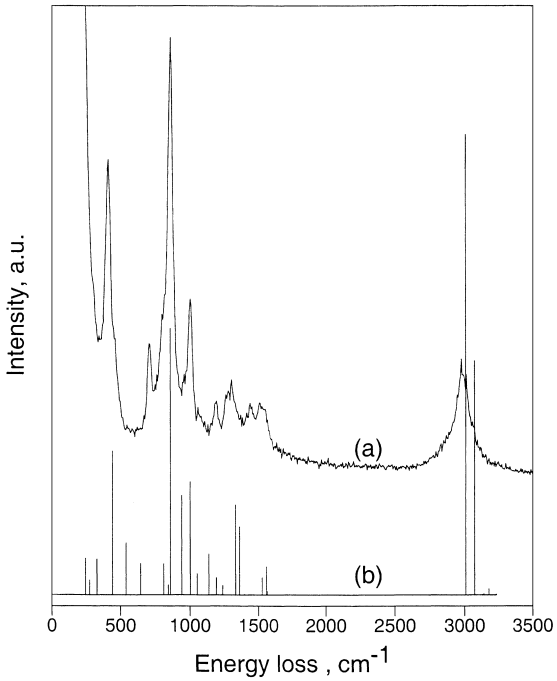


Fig. 9. Comparison between (a) HREEL spectrum collected after EpB exposure to Ag(1 1 0) at 300 K; and (b) IR spectrum calculated for optimized EpB oxametallacycle on a fixed 7-atom cluster.

calculated normal modes for molecular EpB and the 7-atom EpB oxametallacycle structure, respectively. For energy and frequency calculations of molecular EpB, DZ + P basis sets and the BLYP [37] functional were used. Tables 1 and 2 report only the most significant motion for each normal mode; however, many vibrational modes are characterized by simultaneous motion of several parts of the molecule. A more detailed description of the important modes is given here. For the purposes of the following discussion, we treat the HREEL spectrum as the "correct" vibrational spectrum for each adsorbate, and compare theoretically predicted frequencies to experimentally observed spectra. In this work, we refer to the terminal carbon atom on the epoxide ring as the $C^1$ carbon. The other carbon atoms are numbered sequentially, with $C^4$ being the terminal carbon of the vinyl group.

As shown in Table 1, the DFT-predicted vibrational spectrum for EpB is remarkably consistent with both the HREEL spectrum for EpB multilayers adsorbed on Ag(1 1 0) and an IR spectrum of liquid EpB. The observed energy loss at 363 $cm^{-1}$ corresponds to a calculated $C^2$–$C^3$ torsion mode at 330 $cm^{-1}$. The observed 683 $cm^{-1}$ loss is in agreement with a 665 $cm^{-1}$ $C^1$–$C^2$–$C^3$ symmetric deformation mode. The intense doublet at 787 and 806 $cm^{-1}$ conforms to calculated deformations of the epoxide ring at 775 and 779 $cm^{-1}$, respectively. These deformations are caused by out-of-phase and in-phase stretches of C–O bonds. The most intense feature at 917 $cm^{-1}$ is in alignment with two predicted vibrational modes of nearly identical frequency: a $C^1H_2$ twisting mode at

Table 2
Mode assignments and frequency table for EpB oxametallacycle[a]

| Mode | EpB on Ag(1 1 0) at 300 K (HREELS) | Seven-atom fixed cluster (DFT) | Seven-atom non-fixed cluster (DFT) |
|---|---|---|---|
| $\delta_S(O–C^1–C^2)$ | 412 | 442 | 441 |
| $t\omega(C^4H_2)$ | 708 | 646 | 647 |
| $\rho(C^4H_2)$ | 818 | 811 | 827 |
| $\rho(C^4H_2)$ | 861 | 859 | 861 |
| $\omega(C^4H_2)$ | | 942 | 929 |
| $b(C^3H)$ | 1003 | 1002 | 990 |
| $t\omega(C^1H_2)$ | 1193 | 1192 | 1179 |
| $t\omega(C^1H_2)$ | 1279 | 1239 | 1223 |
| $\rho(C^1H_2)$ | 1304 | 1332/1362 | 1319/1341 |
| $\chi(C^4H_2)$[b] | 1452 | | |
| $\chi(C^4H_2)$ | 1507 | 1526 | 1510 |
| $\chi(C^1H_2)$ | 1525 | 1559 | 1541 |
| $\nu_S(C^1–H)$, $\nu_a(C^1–H)$ | 2977 | 3010/3074 | 3008/3073 |
| $\nu_S(C^4–H)$, $\nu_a(C^4–H)$ | 3014 | 3130/3233 | 3129/3232 |

[a] $\tau$: torsion; $t\omega$: twist; $\delta_a$: asymmetric deformation; $\delta_S$: symmetric deformation; $\rho$: rock; $b$: bend; $\nu$: stretch; $\chi$: scissors; $\omega$: wag.
[b] Assigned based on similar mode from molecular EpB spectrum.

910 $cm^{-1}$ and a $C^4H_2$ rocking mode at 918 $cm^{-1}$. The observed energy loss at 996 $cm^{-1}$ corresponds to a predicted 980 $cm^{-1}$ mode which is dominated by $C^3H$ bending, but which also involves bending and twisting of the other CH and $CH_2$ groups. The smaller loss at 1138 $cm^{-1}$ is predicted by a 1118 $cm^{-1}$ vibrational mode dominated by $C^1H$ rocking, but also characterized by bending of the $C^2$–H bond. A predicted $C^1$–$C^2$ stretching mode at 1232 $cm^{-1}$ matches an observed loss peak at 1243 $cm^{-1}$. The losses in the range 1347–1482 $cm^{-1}$ are well-predicted by theoretical $CH_2$ scissors modes. The weak feature at 1654 $cm^{-1}$ corresponds to predicted stretching of the $C^3$–$C^4$ double bond. Finally, the higher-frequency peaks centered near 3000 $cm^{-1}$ correspond to various symmetric and asymmetric stretches of C–H bonds. As demonstrated above and in Table 1, every observed HREELS feature can be accounted for by a theoretically predicted EpB vibrational mode. In conjunction with the IR spectrum of EpB, the excellent agreement between experiment and theory conclusively identifies the species isolated at 140 K as adsorbed molecular EpB. Furthermore, it demonstrates that DFT-based methods can be used to predict vibrational spectra for adsorbed species with a high degree of accuracy.

The key features of the HREEL spectrum collected at 300 K are highly consistent with vibrational modes predicted for the $Ag_7$ EpB oxametallacycle using DFT. The intense mode at 412 $cm^{-1}$ corresponds to a calculated O–C–C deformation at 442 $cm^{-1}$. In this vibration, the oxygen and $C^2$ atoms approach each other in a way that suggests that this mode corresponds to the reaction coordinate for ring-closure to form EpB. The small feature at 708 $cm^{-1}$ is consistent with a predicted $C^4H_2$ twisting mode at 646 $cm^{-1}$. The shoulder at 818 $cm^{-1}$ and the major peak at 861 $cm^{-1}$ are both well-predicted by 811 and 859 $cm^{-1}$ $C^4H_2$ rocking modes. For the 818 $cm^{-1}$ mode, the $C^4H_2$ rocking is in phase with a $C^2H$ bend; for the 861 $cm^{-1}$ mode, the two motions are out of phase. DFT frequency calculations predict a 942 $cm^{-1}$ $C^4H_2$ wagging mode which is not resolved as a loss peak in the experimental HREEL spectrum. DFT calculations do predict a 1002 $cm^{-1}$ $C^3H$ bending mode which is in excellent agreement with the observed loss at 1003 $cm^{-1}$. The observed energy losses at 1193 and 1279 $cm^{-1}$ correspond to predicted $C^1H_2$ twists at 1193 and 1239 $cm^{-1}$, respectively. For the 1239 $cm^{-1}$ mode, this $C^1H_2$ twisting is coupled with some $C^3$–$C^4$ stretching. The loss at 1304 $cm^{-1}$ is consistent with predicted $C^1H_2$ rocking modes at 1332 and 1362 $cm^{-1}$. The small loss observed at 1452 $cm^{-1}$ is not consistent with any features of the theoretical spectrum, but is identical in frequency to one of the $C^4H_2$ scissors modes of EpB, and is therefore assigned as such. The observed features at 1507 and 1525 $cm^{-1}$ correspond to predicted $C^4H_2$ and $C^1H_2$ scissors modes at 1526 and 1559 $cm^{-1}$, respectively. The higher frequency energy losses at approximately 3000 $cm^{-1}$ are assigned to various C–H stretches. Clearly, nearly all of the energy losses observed in the HREEL spectrum are consistent with predictions from DFT-based frequency calculations, conclusively identifying the strongly bound EpB intermediate as a surface oxametallacycle.

## 6. Discussion

In the following discussion, three major topics are addressed. First, the DFT-optimized structure of the EpB oxametallacycle is considered in greater detail, and the link between oxametallacycle structure and reactivity is discussed. Second, the oxametallacycle chemistry observed in this study is compared to previous surface science studies of reactions of epoxides and oxametallacycles. Finally, the implications of this study for the industrial butadiene epoxidation process are considered.

Determining the correct structure for the oxametallacycle involved many cycles of geometry optimizations and frequency calculations. Several energy minima were found for different EpB oxametallacycle geometries, in particular for larger cluster calculations. The oxametallacycle structure shown in Fig. 8 was determined to be the most stable of the various local energy minima; not surprisingly, this structure also yields the best agreement between experimental and calculated vibrational spectra. Previous calculations of oxametallacycle energies indicate that oxametallacycle stability is largely independent of the metal cluster size used for the calculation [18]. This work, however, demonstrates a stronger dependence of the EpB oxametallacycle stabilitv on cluster size. Increasing the silver cluster size from 1 to 7 atoms stabilizes this oxametallacycle by over 13 kcal/mol. Upon inspection of the structure depicted in Fig. 7, it

is easy to understand why increasing the size of the silver metal cluster for this structure has such a strong stabilizing effect. Previous studies of oxametallacycle structure and stability have focused on oxametallacycles bound to a metal dimer (OMMEs). In these structures, the carbon and oxygen ends of the oxametallacycle each interact with only a single atom of the metal dimer. Since the coordination of the oxametallacycle to the surface is fully captured by attachment to a metal dimer, increasing the cluster size has only a small effect on the oxametallacycle energy. For the EpB oxametallacycle of the present study, however, coordination of both the oxygen and $C^2$ carbon atoms to a single silver atom does *not* adequately describe bonding between the adsorbate and the surface. As Fig. 7 demonstrates, more surface atoms are necessary to describe the interaction of the oxametallacycle with the Ag(1 1 0) surface. The oxygen atom is situated in a bridge-bound site between two adjacent silver atoms on a ridge of the (1 1 0) surface. There is also a strong interaction between the terminal ($C^4$) carbon of the vinyl group and a silver atom on the (1 1 0) ridge, with a calculated Ag–$C^4$ bond distance of 2.49 Angstroms. Clearly, at least three silver ridge atoms must be incorporated to properly illustrate the complex interaction between the EpB oxametallacycle and the Ag(1 1 0) surface.

The importance of using larger clusters to describe binding of EpB oxametallacycles has potential implications for the structure sensitivity of reactions involving EpB, including butadiene epoxidation. Previous investigations of oxametallacycles expected to be formed during ethylene epoxidation indicate that coordination to only two Ag atoms fully captures the surface-adsorbate interaction; these observations suggest that reactions involving these oxametallacycles are largely structure insensitive. This is in good agreement with the conclusions reached by Sajkowski and Boudart [38], in their review of the structure sensitivity of ethylene epoxidation.

The larger cluster size required to describe the binding of EpB oxametallacycles, on the other hand, suggests that a greater structure sensitivity may be observed for epoxidation of higher olefins or diolefins. In order to examine the structure sensitivity of EpB oxametallacycle reactions, an examination of the interaction of EpB with the Ag(1 1 1) surface plane is in progress.

The calculated structure of the EpB oxametallacycle on the 7-atom silver cluster may also help explain the reactivity of this intermediate observed during TPD experiments. In carefully considering Fig. 7, one can see that there are actually two cyclic structures in this oxametallacycle configuration. The smaller ring contains the oxygen atom and first two carbon atoms of the chain; i.e. the smaller ring is coordinated to the surface at the O and $C^2$ atoms. The larger ring contains the oxygen atom plus all four carbon atoms in the ring, and is coordinated to the surface at the O and $C^4$ atoms. Closure of the smaller ring (1,2-closure) would result in the formation of EpB as a product. Closure of the larger ring (1,4-closure) would result in the formation of 2,5-DHF. Not surprisingly, EpB and 2,5-DHF are the two products actually observed during TPD of the EpB oxametallacycle. The identification of the strongly-bound EpB intermediate as an oxametallacycle is thus consistent with both our vibrational spectroscopy and TPD results.

Because butadiene epoxidation is a relatively new process [2], the interaction of EpB with single crystal metal surfaces has not yet been studied in detail. Considerable attention, however, has been devoted to the interaction of other epoxides with transition metal surfaces. Ethylene oxide, in particular, has been studied on numerous surfaces, including Ag(1 1 0) [9,31,39], Ag(1 1 1) [40], Cu(1 1 0) [41,42], Pt(1 1 1) [38], Pd(1 1 0) [36,43], Pd(1 1 1) [17], Ni(1 1 1) [44–46], and Rh(1 1 1) [13], among others [47–49]. These studies suggest that ethylene oxide adsorbs to transition metal surfaces through the oxygen atom. It has been found that adsorbed ethylene oxide desorbs without reaction on clean Group IB metal surfaces; the reactivity of these surfaces under UHV conditions is evidently insufficient to induce opening of the epoxide ring. On Group VIII metal surfaces, however, ethylene oxide has been found to undergo ring-opening reactions in which a single C–O bond is broken. Several authors have suggested that decomposition of ethylene oxide on Group VIII metal surfaces proceeds through an oxametallacycle intermediate [13,17,36]. Because oxametallacycles rapidly decompose on Group VIII metal surfaces, however, their isolation and spectroscopic identification has proven difficult. Nonetheless, substantial circumstantial evidence suggests that surface oxametallacycles are formed during decomposition of ethylene oxide.

The reactions of propylene oxide on transition metal surfaces follow similar patterns to the reactions of ethylene oxide. For example, propylene oxide desorbs from clean Ag(1 1 0) without reaction [31]. On Rh(1 1 1), however, propylene oxide decomposes via a pathway analogous to that for ethylene oxide decomposition [13]. Again, ring-opening of propylene oxide appears to proceed through an oxametallacycle intermediate which is insufficiently stable to allow its spectroscopic identification.

We have shown in this study that EpB ring-opens on Ag(1 1 0) to form an oxametallacycle intermediate which is stable over a wide temperature range. As described in the brief literature review above, epoxides in general do not undergo ring-opening on Ag surfaces under UHV conditions. The uniqueness of the EpB ring-opening reaction indicates that an unusually strong driving force exists for the reaction of EpB on Ag(1 1 0) to form an oxametallacycle. This reaction is promoted by the vinyl function of the EpB molecule. It is important to remember that EpB is a bifunctional reagent: both the epoxide and olefin ends of the molecule would be expected to undergo reaction under appropriate conditions. For example, both functions of the EpB molecule are utilized in industrial reactions of EpB [11]. Moreover, as discussed previously, DFT calculations predict a strong interaction between the terminal carbon of the vinyl group and the Ag(1 1 0) surface which significantly enhances the stability of EpB oxametallacycles. Detailed surface science studies of multifunctional reagents on transition metal surfaces are relatively rare. However, the reactions of unsaturated oxygenates such as acrolein, allyl alcohol, and crotonaldehyde have been studied on several transition metal surfaces [50–54]. The vinyl substituent group can open up new reaction channels on these surfaces in addition to the chemistry observed for saturated oxygenates. In the case of EpB, the interaction of the vinyl group with the surface opens up an additional reaction pathway to form 2,5-DHF. Furthermore, multifunctional reagents have been shown in these studies to form adsorbates that are multiply coordinated to the metal surface. This multiple coordination has been shown to have a stabilizing effect on the adsorbed intermediate. In the case of EpB on Ag(1 1 0), interaction of the two functions with the surface appears to have a *combined* effect which results in the formation of a highly stable surface oxametallacycle. Furthermore, the relatively low activity of the Ag(1 1 0) surface for C–C and C–H bond scissions allows the oxametallacycle to remain intact up to a high temperature. Thus, the EpB/Ag(1 1 0) system produces a uniquely stable oxametallacycle that can be synthesized, isolated, and probed spectroscopically.

Because this represents only the second identification of a stable surface oxametallacycle, it is useful to compare the structure and reactivity of the EpB oxametallacycle with the oxametallacycle intermediate previously derived from 2-iodoethanol (IEtOH) on Ag(1 1 0) [10]. The IEtOH-derived oxametallacycle was shown to have an OMME structure; the oxygen and $C^2$-carbon of the adsorbate were bound to either end of a silver dimer, forming a 5-membered ring. In contrast, the EpB oxametallacycle has an OME structure; a common silver atom interacts with the oxygen and $C^2$-carbon of the adsorbate, forming a 4-membered ring. The reactivity of these two oxametallacycles has also been found to be different. IEtOH-derived oxametallacycles were found to undergo cyclization and rearrangement to form γ-butyrolactone (GBL) and acetaldehyde as major products. Importantly, the IEtOH-derived oxametallacycle did not undergo ring-closure to form ethylene oxide. In the present study, however, EpB oxametallacycles have been shown to react via ring-closure to form EpB and 2,5-DHF as products. This represents the first example of ring-closure of a stable surface oxametallacycle to form an epoxide. Based on the differences between reactivity and structure of the limited set of oxametallacycles synthesized to date, one might conclude that an OME oxametallacycle structure is required for ring-closure to form the epoxide. OME structures are more directly analogous to metallaoxetanes proposed as intermediates in epoxide-forming reactions in homogeneous catalysis [55,56]. Furthermore, the EpB OME structure has an intense vibrational mode at ca. $410\,cm^{-1}$ which appears to be the reaction coordinate for ring-closure to form EpB (see above). Although a possible ring-closure mode at $717\,cm^{-1}$ was calculated for the IEtOH-derived OMME, the amplitude of this motion in animations of the vibrations is much less dramatic; furthermore, no mode was observed experimentally at $717\,cm^{-1}$. However, it is not yet clear that oxametallacycles must have the OME structure for ring-closure to be

observed. There are several other differences between the two oxametallacycles isolated to date which might explain differences in reactivity. For example, the vinyl group of the EpB oxametallacycle may suppress the formation of a coupling product analogous to GBL, thus eliminating the bimolecular cyclization pathway. In order to determine which factors control the reactivity of oxametallacycles, further examples of stable oxametallacycles must be identified and studied. Nonetheless, it is clear that oxametallacycles may react via several different pathways, supporting the notion that oxametallacycle intermediates may be implicated in a number of different surface-catalyzed reactions involving oxygenates.

We conclude this section by summarizing the energetics of EpB ring-opening and EpB oxametallacycle ring-closure on Ag(1 1 0), and by underlining parallels between this study and the industrial butadiene epoxidation process. As explained above, we have experimentally determined the activation energy for EpB ring-opening on Ag(1 1 0) to be 8.4 kcal/mol. Using the Redhead analysis [57] assuming a pre-exponential factor of $10^{13}$/s and the experimental TPD heating rate of 1.7 K/s, we have calculated the activation energy for ring-closure of the EpB oxametallacycle to be 32 kcal/mol. These activation energy values are illustrated on the reaction coordinate diagram of Fig. 10. The difference between these two activation energy values is 23 kcal/mol, which corresponds to the heat of reaction for EpB formation from the surface EpB oxametallacycle. This $\Delta H_{rxn}$ was predicted by DFT calculations to be 28.5 kcal/mol on a 7-atom truncation of the Ag(1 1 0) surface and 27.3 kcal/mol on a 12-atom cluster. Thus, the agreement between the experimentally and theoretically predicted $\Delta H_{rxn}$ values is quite reasonable. Both methods of evaluating $\Delta H_{rxn}$ indicate that the EpB oxametallacycle is strongly bound to the surface.

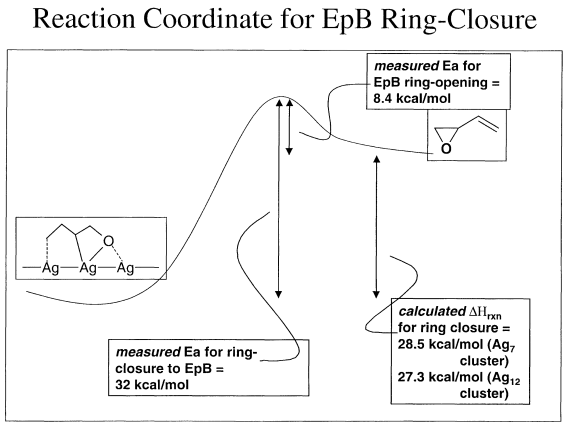


Fig. 10. Schematic of the reaction coordinate for oxametallacycle ring-closure to yield EpB. Activation barriers have been calculated from TPD results; the $\Delta H_{rxn}$ value is calculated for the EpB oxametallacycle on a 7-atom Ag cluster.

The stability of this intermediate suggests that EpB oxametallacycles may be important intermediates in the silver-catalyzed butadiene epoxidation process. It has been reported that EpB formed during this reaction is strongly bound to the silver surface [11]. Given the much higher stability observed in this study for EpB oxametallacycles compared to adsorbed intact EpB, we propose that the strongly bound EpB state reported for the supported catalyst is, in fact, a surface oxametallacycle. In the industrial butadiene epoxidation process, CsCl is added as a promoter; the CsCl promoter increases both the catalytic activity and the selectivity to EpB. It has been reported that CsCl serves to lower the apparent activation energy for EpB formation to 26 kcal/mol by lowering the desorption energy of EpB [11]. This value is in excellent agreement with our predicted value for the $\Delta H_{rxn}$ of EpB oxametallacycles, suggesting that CsCl may function by lowering the activation barrier for oxametallacycle ring-closure to near its thermodynamically-limited value; i.e. the activation energy for ring-opening of EpB is lowered to near zero. The demonstration of the connection between oxametallacycle intermediates and epoxide molecules has been facilitated in the present study by the high stability of the EpB oxametallacycle intermediate. However, the strong similarity between the butadiene epoxidation process and the epoxidation processes of other olefins (notably ethylene) suggests that oxametallacycles may be universally important intermediates in silver-catalyzed olefin epoxidation.

## 7. Conclusions

Epoxybutene adsorbed on Ag(1 1 0) at moderate temperature undergoes ring-opening to produce a highly stable surface oxametallacycle. The excellent agreement between experimental HREEL and DFT-predicted IR spectra of this intermediate conclusively

identifies the oxametallacycle structure. This oxametallacycle undergoes ring-closure reaction at 490 K to reform EpB; vibrational spectroscopic studies reveal a vibrational mode at 412 $cm^{-1}$ which appears to correspond to the reaction coordinate for this ring-closure. DFT calculations indicate a strong interaction between the terminal C atom of the oxametallacycle vinyl group and the surface; this interaction stabilizes the oxametallacycle and opens up a reaction pathway for production of small amounts of 2,5-DHF at 510 K. These results represent the first example of ring-opening of an epoxide to form a stable surface oxametallacycle, and the first demonstration of oxametallacycle ring closure to form an epoxide. Further, the high stability of the oxametallacycle produced from EpB in this study suggests that the strongly bound state reported for EpB on supported butadiene epoxidation catalysts is a stable oxametallacycle intermediate. The link between oxametallacycle intermediates and epoxide products shown here has implications for the mechanism of olefin epoxidation in general, including ethylene epoxidation.

## Acknowledgements

The silver-catalyzed epoxidation of olefins, reviewed by Professor Boudart in reference [38], has been a favorite topic of many members of his "school". As his second and third generation academic "descendants", we are pleased to trace our interest in this subject to Bob Madix and Michel Boudart, and to their influence on one of us (MAB) at Stanford and thereafter.

We also gratefully acknowledge the financial support (Grant FG02-84ER13290) for this research by the U.S. Department of Energy, Office of Science, Division of Chemical Sciences. JWM acknowledges the National Science Foundation for financial assistance in the form of a graduate fellowship. Finally, the assistance of Dr. Hok-Tsan Lam and Katy Lee in collecting the HREEL spectra, and of Dr. Markus Kinne in collecting IR spectra, was highly appreciated.

## References

[1] Chem. Eng. News 74 (1996) 17.
[2] D. Denton, J. Monnier, S. Falling, J. Stavinoha, W. Watkins, Chim. Org. 5 (1996) 17.
[3] R.A. van Santen, H.P.C. Kuipers, Adv. Catal. 35 (1987) 265.
[4] J.G. Serafin, A.C. Liu, S.R. Seyedmonir, J. Mol. Catal. 131 (1998) 157.
[5] R.B. Grant, R.M. Lambert, J. Catal. 92 (1985) 364.
[6] S. Hawker, C. Mukoid, J.P.S. Badyal, R.M. Lambert, Surf. Sci. 219 (1989) L615.
[7] J.T. Roberts, R.J. Madix, J. Am. Chem. Soc. 110 (1988) 8540.
[8] C. Mukoid, J.P.S. Badyal, R.M. Hawker, S. Lambert, Catal. Lett. 4 (1990) 57.
[9] C. Backx, C.P.M. De Groot, P. Biloen, W.M.H. Sachtler, Surf. Sci. 128 (1983) 81.
[10] G.S. Jones, M. Mavrikakis, M.A. Barteau, J.M. Vohs, J. Am. Chem. Soc. 110 (1998) 3196.
[11] J. Monnier, Stud. Surf. Sci. Catal. 110 (1997) 135.
[12] R.L. Brainard, R.J. Madix, J. Am. Chem. Soc. 111 (1989) 3826.
[13] N.F. Brown, M.A. Barteau, Surf. Sci. 298 (1998) 6.
[14] C.J. Houtman, M.A. Barteau, J. Catal. 130 (1991) 528.
[15] X. Xu, C.M. Friend, J. Am. Chem. Soc. 113 (1991) 6779.
[16] R. Shekhar, M.A. Barteau, J. Vac. Sci. Technol. A 14 (1996) 1469.
[17] R.M. Lambert, R.M. Ormerod, W.T. Tysoe, Langmuir 10 (1994) 730.
[18] M. Mavrikakis, D.J. Doren, M.A. Barteau, J. Phys. Chem. B 102 (1998) 394.
[19] J.W. Medlin, M. Mavrikakis, M.A. Barteau, J. Phys. Chem. B 103 (1999) 11169.
[20] J.T. Roberts, R.J. Madix, A.J. Capote, J. Am. Chem. Soc. 113 (1991) 9848.
[21] J.L. Davis, M.A. Barteau, Surf. Sci. 208 (1989) 383.
[22] R.V. Plank, J.M. Vohs, Surf. Sci. 340 (1995) L971.
[23] E.I. Ko, R.J. Madix, J.B. Benziger, J. Catal. 62 (1980) 264.
[24] G.S. Jones, M.A. Barteau, J.M. Vohs, Surf. Sci. 420 (1999) 65.
[25] E.J. Baerends, D.E. Elis, P. Ros, Chem. Phys. 2 (1973) 41.
[26] E.J. Baerends, P. Ros, Quant. Chem. Symp. 12 (1978) 169.
[27] P.M. Boerrigter, G. te Velde, E.J. Baerends, Int. J. Quant. Chem. 33 (1988) 87.
[28] S.H. Vosko, L. Wilk, M. Nusair, Can. J. Phys. 58 (1980) 1200.
[29] A.D. Becke, Phys. Rev. A 38 (1988) 3098.
[30] J.P. Perdew, Phys. Rev. B 33 (1986) 8822.
[31] S.R. Bare, J. Vac. Sci. Technol. A 10 (1992) 2336.
[32] X. Xu, C.M. Friend, Surf. Sci. 260 (1992) 14.
[33] X. Xu, C.M. Friend, J. Phys. Chem. 95 (1991) 10753.
[34] N.F. Brown, M.A. Barteau, Langmuir 8 (1992) 862.
[35] N.F. Brown, M.A. Barteau, J. Phys. Chem. 100 (1996) 2269.
[36] R. Shekhar, M.A. Barteau, Surf. Sci. 348 (1996) 55.
[37] C.T. Lee, W.T. Yang, R.G. Parr, Phys. Rev. B 37 (1988) 785.
[38] D.J. Sajkowski, M. Boudart, Catal. Rev. Sci. Eng. 29 (1987) 325.
[39] C.T. Campbell, M.T. Paffett, Surf. Sci. 177 (1986) 417.
[40] R.B. Grant, R.M. Lambert, J. Catal. 93 (1985) 92.
[41] C. Benndorf, B. Kruger, B. Nieber, Appl. Catal. 25 (1986) 165.
[42] C. Benndorf, B. Nieber, J. Vac. Sci. Technol. 4 (1986) 1355.

[43] R. Shekhar, M.A. Barteau, R.V. Plank, J.M. Vohs, Surf. Sci. 384 (1997) L815.
[44] B. Nieber, C. Benndorf, J. Vac. Sci. Technol. 8 (1990) 2431.
[45] B. Nieber, C. Benndorf, Surf. Sci. 269/270 (1992) 341.
[46] B. Nieber, C. Benndorf, Surf. Sci. 235 (1990) 129.
[47] C. Benndorf, B. Nieber, B. Kruger, Surf. Sci. 189/190 (1987) 511.
[48] J.G. Serafin, C.M. Friend, J. Am. Chem. Soc. 111 (1989) 6019.
[49] M. Weinelt, P. Zebisch, H.P. Steinruck, Surf. Sci. 287/288 (1993) 471.
[50] J.L. Davis, M.A. Barteau, J. Mol. Catal. 77 (1992) 109.
[51] N.F. Brown, M.A. Barteau, J. Am. Chem. Soc. 114 (1992) 4258.
[52] F. Delbecq, P. Sautet, J. Catal. 152 (1995) 217.
[53] J.C. de Jesus, F. Zaera, J. Mol. Catal. A 138 (1999) 237.
[54] J.C. de Jesus, F. Zaera, Surf. Sci. 430 (1999) 99.
[55] K.A. Jorgensen, B. Schiott, Chem. Rev. 90 (1990) 1483.
[56] K.B. Sharpless, A.Y. Teranashi, J.E. Backvall, J. Am. Chem. Soc. 99 (1977) 3120.
[57] P.A. Redhead, Vacuum 12 (1962) 203.